Physics – Uspekhi **64** (2) 141 – 156 (2021)

REVIEWS OF TOPICAL PROBLEMS

PACS numbers: **01.65.+g**, 24.30.Cz, **25.20.–x**

Giant dipole resonance of atomic nuclei. Prediction, discovery, and research

B S Ishkhanov, I M Kapitonov

DOI: https://doi.org/10.3367/UFNe.2020.02.038725

Contents

Abstract. Three quarters of a century ago, in his paper "Quadrupole and dipole γ-emission from nuclei" [*J. Phys. USSR* 8 331 (1944); *Zh. Eksp. Teor. Fiz.* 15 81 (1945)], A B Migdal introduced the concept of quantum collective excitation modes into nuclear physics, thereby predicting the phenomenon of giant dipole resonance (GDR). GDR research has had an enormous influence on the formation of modern concepts relating to the dynamics of nuclei. We briefly discuss Migdal's paper and trace the history of theoretical and experimental studies of GDR. New forms of GDR and analogues of GDR in nonnuclear microsystems are mentioned.

Keywords: giant dipole resonance, collective excitation modes, photonuclear reactions, nuclear physics

Dedicated to the 75th anniversary of A B Migdal's work "Quadrupole and dipole γ-emission from nuclei"

1. Introduction. Prediction of giant dipole resonance

The year 2020 marks the 75th anniversary of the publication of A B Migdal's pivotal paper, "Quadrupole and dipole γ-emission from nuclei" [1], in which he predicted the existence of collective excitations of a new type in atomic nuclei. In contrast to less energetic surface oscillations of the nuclear liquid droplet, the oscillations predicted by Migdal involve all nucleons of the nucleus. In the process of these oscillations, all the neutrons move with respect to all the protons, generating electric dipole excitations with energies >10 MeV. This was in fact a prediction of the important universal nuclear phenomenon — the giant dipole resonance (GDR) that is dominant in cross sections of photon absorption by atomic nuclei caused by electric-dipole E1-photons.

The magnitude of this phenomenon on the scale of nuclear and nucleon excitation energies is shown schematically in Fig. 1. GDR, inherent in all nuclei with the number of nucleons $A > 2$, is the strongest response of atomic nuclei to electromagnetic radiation. It dominates in the energy range 10–50 MeV, covering nearly half the energy scale of nuclear excitations that extends to approximately 100 MeV.

In [1], Migdal evaluated the dipole moment d induced in a nucleus under the action of a uniform external field. He used the semiclassical analysis based on the notion of mutually permeating proton and neutron liquids. Invoking the sum rule for electric dipole transitions and barely relying on specific models, Migdal obtained a relation between the average energy $\langle E \rangle$ of these transitions and the constant β in the symmetry energy term $\beta (N-Z)^2/A$ in Weizsäcker's semiempirical formula for the binding energy of the nuclear

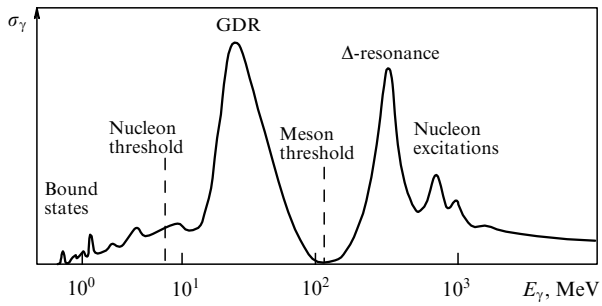

Figure 1. Schematic dependence of the cross section of photon absorption by atomic nuclei and free nucleons on the photon energy.

B S Ishkhanov [(1)], **I M Kapitonov** [(2)].
Lomonosov Moscow State University, Department of Physics, Leninskie gory 1, str. 2, 119991 Moscow, Russian Federation
E-mail: [(1)] bsi@depni.sinp.msu.ru, [(2)] igor-kapitonov@yandex.ru

Received 25 December 2019, revised 27 January 2020
Uspekhi Fizicheskikh Nauk **191** (2) 147 – 162 (2021)
Translated by S Alekseev

liquid droplet:

$$E_{\rm b} = \alpha A - \beta \frac{(N-Z)^2}{A} - \gamma A^{2/3} - \eta \frac{Z(Z-1)}{A^{1/3}} + \varepsilon \frac{(-1)^N + (-1)^Z}{A^{3/4}}, \quad (1)$$

where N and Z are the numbers of neutrons and protons in a nucleus, and α, β, γ, η, and ε are empirically chosen numerical coefficients. Migdal assumed that the energy is distributed uniformly over the entire nucleus and is characterized by the density $\beta(\rho_{\rm n} - \rho_{\rm p})^2/\rho$, where $\rho_{\rm n}$, $\rho_{\rm p}$, and ρ are the respective densities of the neutron and proton liquids and the total density ($\rho_{\rm n} + \rho_{\rm p} = \rho = \text{const}$).

The calculation procedure amounted to equating the static dipole moment of the nucleus in a uniform electric field, calculated using Weizsäcker's formula for a small volume of nuclear matter, with the quantum mechanical expression for the dipole moment. The resultant relation allowed finding the average energy $\langle E \rangle$ of dipole transitions:

$$\frac{\sum_n |d_{0n}|^2/(E_n - E_0)}{\sum_n (E_n - E_0)|d_{0n}|^2} = \frac{1}{\langle E \rangle^2}, \quad (2)$$

where d_{0n} is the static dipole moment acquired by the nucleus under the transition from the ground state with the energy E_0 to an excited state with the energy E_n. The numerator on the left-hand side of relation (2) is expressed in terms of the static dipole moment d calculated by Migdal using Weizsäcker's formula, and the denominator is evaluated with the help of the dipole sum rule $\sum_n (E_n - E_0)|d_{0n}|^2$ using its classical expression $[2\pi^2 e^2 \hbar/(Mc)]Z$, where M is the nucleon mass. The average energy $\langle E \rangle$ of dipole excitations evaluated by Migdal can be written in the form

$$\langle E \rangle = \sqrt{40 \frac{NZ}{A^2} \beta \frac{\hbar^2}{MR^2}} \approx 80 A^{-1/3} \text{ MeV}. \quad (3)$$

For numerical estimates, we here take the value $\beta = 24$ MeV and the nucleus radius $R = 1.2A^{1/3}$ fm. For heavy nuclei, formula (3) then gives $\langle E \rangle = 13-14$ MeV. We note that although Migdal's calculations were based on the collective model of proton and neutron liquids, they are equally well applicable to the shell model of two ideal Fermi gases.

2. Giant dipole resonance as a collective nuclear excitation

Giant dipole resonance was first observed in 1947 and 1948 in two experiments by Baldwin and Klaiber [3] on a betatron bremsstrahlung γ-beam with the energy of 100 MeV. Baldwin and Klaiber discovered that the cross sections of the $^{12}{\rm C}(\gamma, {\rm n})$ and $^{63}{\rm Cu}(\gamma, {\rm n})$ reactions and the Th photofission reaction have wide maxima centered at the energies of 16–25 MeV.

The results of these measurements were interpreted by Goldhaber and Teller [4], who were apparently unaware of Migdal's work. Independently of Migdal, the authors of [4] noted the electric dipole character of photon absorption in the energy range 10–30 MeV and obtained expressions for the resonance energy $E_{\rm m}$ of classical harmonic oscillations of protons with respect to neutrons in three approximations:

(1) each proton and each neutron oscillates about its equilibrium position, similarly to ions vibrating in a crystal;

(2) protons and neutrons oscillate with respect to each other similarly to compressible liquids within the fixed surfaces of the nucleus (Migdal's version);

(3) protons and neutrons oscillate with respect to each other similarly to hard (incompressible) spheres.

According to the first model, $E_{\rm m}$ is independent of the number A of nucleons in the nucleus; according to the second model, it is proportional to $A^{-1/3}$; and according to the third, it is proportional to $A^{-1/6}$. Because the best correspondence with experiment at the time followed for $E_{\rm m} \sim A^{-1/6}$, Goldhaber and Teller developed a third model, which in the literature has since been associated with their names. According to the Goldhaber–Teller model, $E_{\rm m} \approx 45A^{-1/6}$ MeV.

The second model proposed by Goldhaber and Teller, i.e., Migdal's model of compressible proton and neutron liquids, was developed by Steinwedel and Jensen [5], and also by Danos [6]. Just as Migdal did, the authors of [5, 6] wrote the density of the symmetry energy of the nucleus as $\beta(\rho_{\rm n} - \rho_{\rm p})^2/\rho$. The external electromagnetic field induces reverse-phase oscillations of the neutron and proton liquid densities (polarization oscillations), which satisfy the usual wave equation of hydrodynamics. The wave number of such oscillations is related to the symmetry energy constant β. Sound waves of a certain type (so-called second sound waves) occur in the nucleus, such that the two nucleon liquids oscillate with respect to each other, and the total density of the nucleons is assumed to be constant.

Detailed calculations of the lowest resonance frequency of these oscillations leads to the following expression for the resonance energy $E_{\rm m}$:

$$E_{\rm m} = \sqrt{34.6 \frac{NZ}{A^2} \beta \frac{\hbar^2}{MR^2}} \approx 75 A^{-1/3} \text{ MeV}. \quad (4)$$

We can see that, despite the use of more sophisticated mathematical tools, the obtained relation virtually reproduces relation (3) that follows from Migdal's approach.

We compare the predictions that the Migdal model and the Goldhaber–Teller model of hard nucleon spheres make for the position of the GDR maximum $E_{\rm m}$ as a function of the mass number A with experimental date available for most of the stable nuclei, some of which are presented in Fig. 2. We can see that, as A increases, the GDR maximum $E_{\rm m}$ moves to lower energies. The corresponding experimental dependence is shown with dots in Fig. 3, to be compared with the predictions of the two models under discussion. The choice in favor of the Migdal model is evident: this model is especially good at reproducing the experimental data in the range of A from 50 to 150. Thus, in the framework of the collective approach, GDR is to be treated as reverse-phase oscillations of compressible proton and neutron liquids within the fixed nucleus surface, rather than relative oscillations of two hard nucleon spheres.

In 1958, Danos [6] and Okamoto [7] established the existence of a correlation between the GDR width Γ and the quadrupole deformation parameter δ for the nucleus in the ground state (the Danos–Okamoto effect). The essence of this effect is that in nonspherical nuclei shaped like an axially symmetric ellipsoid there must be two resonance frequencies of dipole oscillations (which means splitting into two GDR components) corresponding to motions of the oscillating liquids along and across the nucleus symmetry axis. This must lead to a broadening of the photoabsorption cross

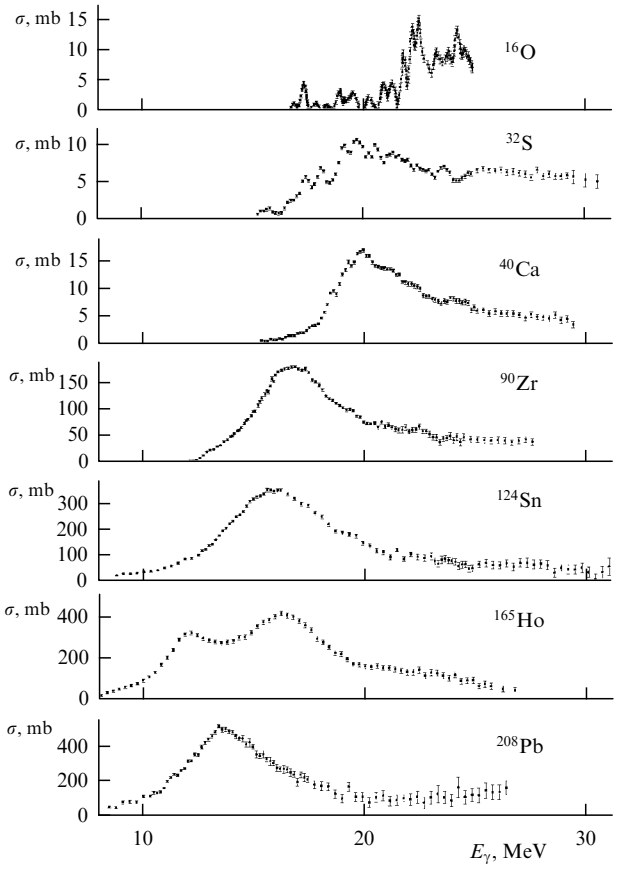

Figure 2. Cross section of the photoneutron reaction in the GDR domain on nuclei with different mass numbers A.

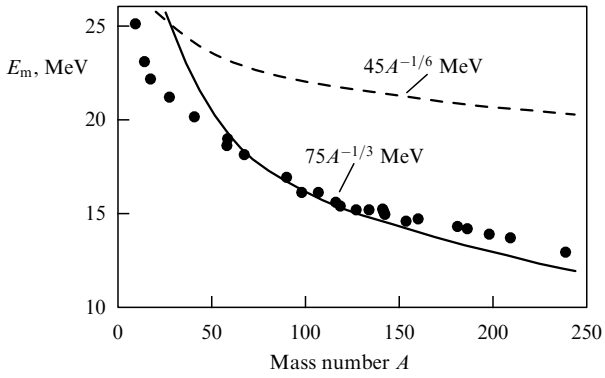

Figure 3. Experimental dependence of the GDR maximum E_m on the mass number A (dots) and predictions of the Migdal (Steinwedel–Jensen) model, solid line, and the Goldhaber–Teller model, dotted line.

section and, at large deformations, to the appearance of two maxima in it. The lower-energy maximum must then correspond to dipole vibrations along the major axis of the nuclear ellipsoid, and the higher-energy maximum, to vibrations along the minor axis. As an example, in Fig. 4 we show the 1974 data on cross sections of photoneutron reactions of an isotope of samarium [8].

We can clearly see that, as A increases, the GDR first broadens and then splits into two maxima, which means the formation of two giant resonance components.

The appearance of two GDR components in axial nuclei with pronounced quadrupole deformation is an effect predicted by the Migdal model. Indeed, it follows from

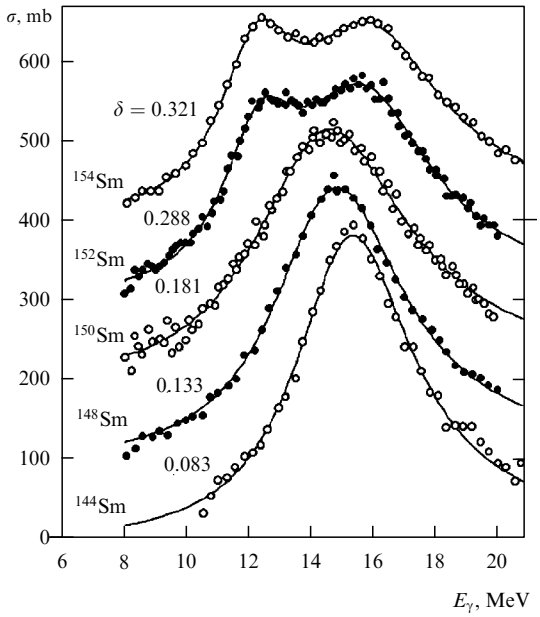

Figure 4. Photoneutron cross section of Sm isotopes [8]. Values of their quadrupole deformation parameter δ are given.

formulas (3) and (4) that the resonance energy (frequency) of dipole oscillations is inversely proportional to the nucleus radius R. An axial nucleus has two characteristic sizes: the respective lengths a and b of the minor and major axes of the ellipsoid, and therefore their resonance energies must be shifted by the quantity

$$\Delta E = E_a - E_b \approx 75 \times 1.2\left(\frac{1}{a} - \frac{1}{b}\right) \text{ MeV} \approx 75A^{-1/3}|\delta| \text{ MeV}, \quad (5)$$

with the deformation parameter $\delta = (b-a)/\langle R\rangle$ and with $\langle R\rangle = \sqrt{ab} = 1.2A^{1/3}$ fm. Formula (5) reproduces to within 10 to 15% the GDR splitting magnitude for the heaviest isotopes of samarium, ^{152}Sm and ^{154}Sm.

The GDR splitting into two components is also clearly manifested in the strongly deformed nucleus ^{165}Ho, for which $|\delta| = 0.294$ (see Fig. 2). The magnitude of this splitting coincides with the one estimated by formula (5) to within 5%. These data, along with some others pertaining to heavy deformed nuclei, on the one hand suggest that the nonsphericity degree of these nuclei is preserved at excitation energies of 10–20 MeV, and on the other hand are evidence in support of the Migdal model.

3. First stage of experimental giant dipole resonance studies

Migdal and his collaborators returned to the description of GDR 20 years after the appearance of his pioneering work [1], armed with the theory of finite Fermi systems (TFFS) that he had developed [9–12]. By that time, GDR studies were in full swing. Immediately after its experimental discovery, this phenomenon attracted the attention of nuclear physicists, and they set about studying it. Several dozen laboratories across the world included GDR investigations on the list of their high-priority research tasks, which was facilitated by the appearance of accessible electron accelerators at energies up to 100 MeV, such as betatrons, synchrotrons, linear accel-

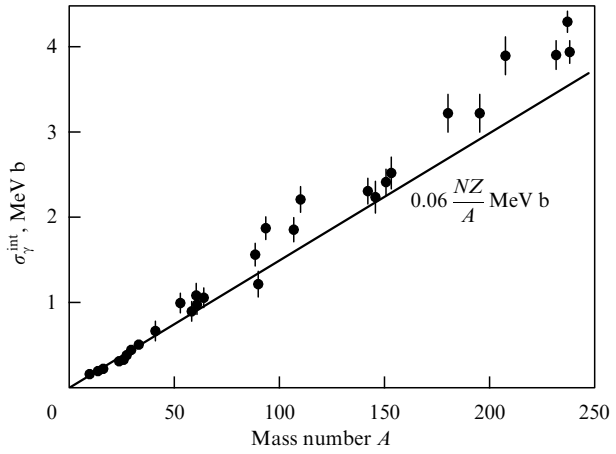

Figure 5. Integral photoabsorption cross sections in the GDR range for nuclei with different mass numbers. Line: prediction of the classical dipole sum rule.

erators, and microtrons. The most active and successful experimental investigations were performed in the USA, Canada, the USSR, Germany, France, Italy, the Netherlands, Belgium, Sweden, Yugoslavia, and Australia. In the focus of investigations were the cross sections of the main GDR decay channels, the photoproton and photoneutron ones, and, less frequently, the total photon absorption cross section and, the spectrum and angular distribution of photonucleons. Data for the most abundant stable isotopes were obtained rather quickly, confirming that GDR is a major and universal nuclear phenomenon caused by electric-dipole photons.

In Figure 5, we show the photoabsorption cross sections integrated over the GDR range $\sigma_\gamma^{\rm int} = \int \sigma_\gamma(E_\gamma)\,{\rm d}E_\gamma$ for nuclei with various numbers of nucleons; the cross sections were obtained both by summing the cross sections of the main photonucleon reactions and by using the direct measurements of photoabsorption cross sections. That the classical estimate $0.06(NZ/A)$ MeV b is close to the experimental values proves the electric dipole nature of the photons absorbed by the nucleus. In the case of dominant absorption of other types of photons (M1, E2, ...), experimental values agreeing with the long-wavelength approximation (photon wavelengths $\lambda \gg R$, where R is the nucleus radius) would have been positioned much lower than the classical estimates. That the experimental values are somewhat (up to $\approx 30-40\%$) higher than the estimate $0.06(NZ/A)$ MeV b for nuclei with $A > 100$ can be explained by the particular properties of internucleon forces, first and foremost by their exchange nature [13].

Conducting photonuclear experiments on electron accelerators turned out to be challenging. Besides overcoming the difficulties due to the small cross sections of photonuclear reactions, methods for using electron beams to generate high-energy photons had to be worked out. The most frequently used way of generating such photons is the production of bremsstrahlung γ-radiation beams. Most (and at the initial stage of investigations, overwhelmingly most) of the photonuclear experiments were conducted with the help of bremsstrahlung beams. But because the bremsstrahlung γ-radiation spectrum is continuous, with the upper edge $E_\gamma^{\rm max}$, the immediate result of an experiment is not the reaction cross section but the yield $Y(E_\gamma^{\rm max})$ related to the effective cross section $\sigma(E_\gamma)$ by the integral equation

$$Y(E_\gamma^{\rm max}) = \int_0^{E_\gamma^{\rm max}} \sigma(E_\gamma) W(E_\gamma, E_\gamma^{\rm max})\,{\rm d}E_\gamma\,, \qquad (6)$$

where the integrand contains the product of the spectral function of bremsstrahlung radiation $W(E_\gamma, E_\gamma^{\rm max})$ and the reaction cross section. The integration over energy ranges all energies of bremsstrahlung photons (from 0 to $E_\gamma^{\rm max}$). The strategy to find $\sigma(E_\gamma)$ is to measure the reaction yield at different upper edges of the bremsstrahlung spectrum and then to solve the so-called inverse problem (finding $\sigma(E_\gamma)$), given the dependence of the yield on $E_\gamma^{\rm max}$, by some numerical integration method. The intricate details of work with bremsstrahlung radiation beams and the methods for extracting cross sections from the yield curves are available in [14–21].

In the USSR, the first measurements of photonuclear reaction cross sections on a bremsstrahlung γ-radiation beam were done in 1949–1950. The photofission cross sections of uranium (^{233}U, ^{235}U, and ^{238}U) and thorium (^{232}Th) isotopes were obtained [22]. The measurements were made at the Physical Institute of the USSR Academy of Sciences (FIAN) on a 30-MeV synchrotron constructed under the supervision of V I Veksler. A differential ionization chamber was used to register the fission products. The measurements showed that all the cross sections obtained are similar in shape and have distinct maxima at the energy of 13–14 MeV. The position and shape of these cross sections turned out to be similar to the cross sections of other photonuclear reactions on the same nuclei.

In the 1950s, investigations of cross sections of photoneutron reactions on intermediate-mass and heavy nuclei were underway across the world, which was explained by a relatively larger $(\gamma, {\rm n})$ reaction cross section on these nuclei than the cross sections of other photonuclear reactions, as well as by the possibility of using thick targets. In addition, the background could be minimized by time-separating the processes of target irradiation by γ-quanta pulses and of neutron registration if decelerating detectors or the method of induced activity were used. A major contribution to these investigations was made by the studies conducted at FIAN. The photoneutron production cross sections of ten intermediate-mass and heavy elements (Cu, Zn, Cd, I, Ta, Au, Tl, Bi, Th, U) were measured [23]. All the cross sections had the shape of giant resonances. Integrated cross sections were in agreement with the estimates based on sum rules [13].

In the same period, the 30-MeV synchrotron at FIAN was used to measure energies and angular distributions of photoprotons in nuclei of copper, nickel, and other intermediate-mass nuclei with the help of nuclear photographic emulsions, which showed a significant excess in the photoproton yield compared with the one predicted by the evaporation model in the high-energy end of the proton spectrum [24, 25].

A major contribution to the knowledge about GDR was made by direct measurements of the total cross section of the photon absorption by nuclei made at FIAN in 1962–1981. The essence of the method (the first iteration of its use being described in [26]) is to measure the attenuation of a photon beam of bremsstrahlung radiation that has passed through an absorbent with a known thickness containing the nuclei in question and to compare it with the original beam to find the total cross section of all interaction processes (both nuclear

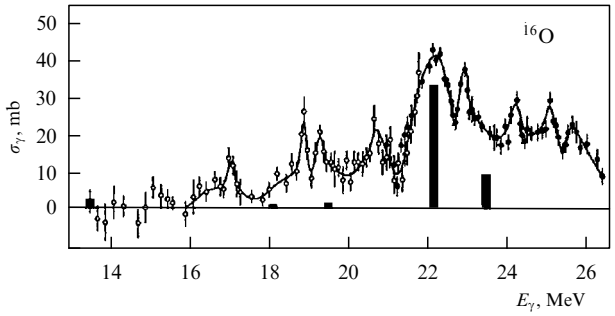

Figure 6. Photoabsorption cross section for the ^{16}O nucleus, measured using the direct method on a 250-MeV synchrotron [27, 28]. Columns: data from the calculations in [41].

and nonnuclear) of atoms of the investigated substance with γ-quanta. Because the nonnuclear processes are studied well, their contribution to the total cross section can be subtracted and the result attributed to nuclear photoabsorption. The use of a γ-spectrometer allowed bypassing the complications due to the continuous nature of the bremsstrahlung radiation spectrum, and the energy resolution of the method was entirely determined by the quality of the γ-spectrometer. In the experiments at FIAN, the photon detector was chosen as a pair magnetic spectrometer with a 120-keV resolution for 20-MeV photons and efficiency of $\approx 10^{-6}$.

The result for the ^{16}O nucleus is presented in Fig. 6, which shows a distinct structure in the photoabsorption cross section of the nucleus. Similarly, work by the photonuclear group in Ljubljana (Yugoslavia), who were also using the method of total photoabsorption but with a Compton spectrometer, revealed essential features in the nuclear photoabsorption cross sections for some nuclei, from beryllium to calcium [29, 30]. This method has thus confirmed the existence of an intricate GDR structure observed in a number of earlier photoneutron experiments.

At FIAN in the 1960s, the method of total photoabsorption was used to obtain not only the ^{16}O cross sections but also those for ^{9}Be, ^{12}C, ^{19}F, ^{24}Mg, ^{27}Al, ^{32}S, ^{40}Ca, and Fe nuclei. Later, in 1974–1981, more than 20 intermediate-mass and heavy nuclei were investigated, also showing the Danos–Okamoto effect for deformed nuclei.

The first stage of studies of GDR continued for one and a half decades after its experimental discovery. The most general GDR characteristics were obtained during that period. The range of the GDR energy position and the cross sections were determined for many nuclei (mainly in photoneutron reactions). The GDR structure transpired in some photoneutron experiments and also in measuring the photoabsorption and inverse photonuclear reaction cross sections. The energy and angle distributions of photoprotons averaged over the bremsstrahlung spectrum were measured for a number of nuclei. Bremsstrahlung γ radiation was used in virtually all experiments.

Since the 1960s, the experimental capabilities of photonuclear investigations have been steadily growing. Experiments have become possible that result in deeper insights into the GDR formation and decay mechanism. Before proceeding to the data of a new generation of experimental studies, we briefly discuss the status of theoretical GDR investigations existing at the time. A more detailed review of theoretical concepts pertaining to GDR, with more references, can be found in [15, 31, 32, 55].

4. Theoretical giant dipole resonance investigations. A microscopic approach

Along with the development and wide use of the concept of collective forms of motion in nuclei, the ideas of independent motion of nucleons and the essential role played by one-particle degrees of freedom were shaped by the early 1950s [33]. It has become possible to interpret the GDR within a microscopic approach. The first attempts to explain the phenomenon of GDR that way were already made in 1953 (references to earlier works can be found in [34]). This approach was most fully implemented by Wilkinson [35]. It was shown that in the one-particle shell model the electric dipole excitations are formed by transitions of nucleons from the filled shell to the nearest unoccupied shell, and therefore their energy is close to the mean separation between the shells. These transitions are grouped within a relatively narrow energy range determined by the spread of E1-transition energies; the GDR thus also occurs in this approach. It was therefore assumed that GDR forms from noninteracting one-particle–one-hole (1p1h) nucleon configurations (where p is a nucleon in the free shell and h is the vacancy (hole) in the filled shell) and its 'collective' features are absent. It then turned out that the calculated GDR energy was much lower (in heavy nuclei, by a factor of two) than the experimentally observed one.

The descriptions of GDR in collective models and in the model of independent particles located in the mean nuclear field were apparently mutually exclusive. However, it was shown in [36] that in the oscillator mean field, the dipole 1p1h configurations can be used to construct a coherent superposition that reproduces the oscillatory motion of the centers of mass of protons and neutrons in collective models. The situation was clarified with the appearance of studies [37–39]. In the first of these, the example of GDR in the ^{16}O nucleus was used to show that taking residual nucleon–nucleon forces into account in the shell model shifts the dipole excitation energy toward larger values, thus eliminating the major drawback of the one-particle model, the GDR maximum being positioned too low.

The role of the residual interaction in the formation of GDR in light nuclei was also investigated in [38]. The effect of residual forces was analyzed by Brown and Bolsterly [39], who demonstrated that, due to accumulation effects, these relatively weak forces lead to the formation of a coherent state with correlated motion of a large number of nucleons from independent 1p1h configurations. The major part of the dipole force is then accumulated in a single coherent resonance, which draws the results of shell-model calculations closer to the results of the collective approach, predicting the excitation of one collective degree of freedom of the nucleus: proton–neutron oscillations.

We can say that, in interpreting GDR, the formation mechanism of collective excitations at the microscopic level was revealed. Subsequently, many GDR calculations were done within the 1p1h approximation of the shell model with different forms of residual interaction. The E1 transition strengths that follow from the calculations in [41] and [40] are respectively shown (in relative units) in Fig. 6 for ^{16}O and in Fig. 7 for ^{208}Pb.

Among the different versions of 1p1h calculations, the most popular were the random phase approximation (RPA) [42], the TFFS [9–12], and the method of coupled channels [43]; despite the different assumptions, all three led

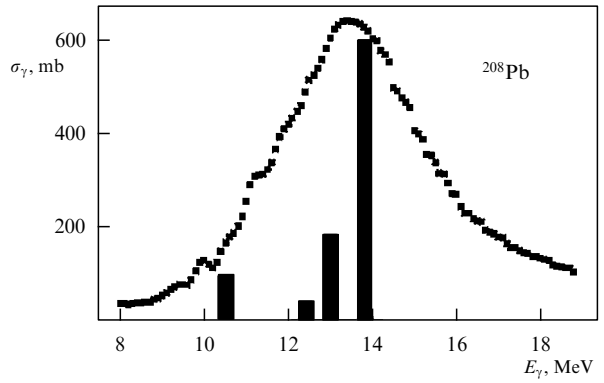

Figure 7. Squares: photoabsorption cross section for the ^{208}Pb nucleus obtained by summing all the experimental photonucleon cross sections. Columns: data from the calculations in [40].

to approximately the same results. After replacing particles and holes with quasiparticles, the 1p1h approach becomes applicable not only to closed-shell nuclei but also to intermediate-mass and heavy spherical nuclei with unfilled shells, as well as to strongly deformed nuclei. In the last case, the description of one-particle motion involves a deformed one-particle potential, and the GDR splits into two maximums corresponding to neutron-proton oscillations along and across the nucleus symmetry axis, in accordance with predictions of the collective hydrodynamics model [6, 7]. An essential step in advancing the 1p1h approach was made in [43–45], where calculations were extended to the continuum, which allowed, first, describing the GDR decay as a result of a particle escaping to the continuous spectrum and, second, taking the effects due to the interference of close resonances into account.

It turned out at the same time that most of the RPA calculations, even with the continuum taken into account, do not describe the GDR structure and width. We let Γ_Δ denote the GDR width, which we understand as the range of energy spread of most of the photoabsorption cross section σ_γ, i.e., the width of the photoabsorption domain. It ranges from 4 to 20 MeV and shows no apparent trend as A increases. Moreover, changing the number of nucleons in a nucleus by 1 or 2 can lead to a dramatic change in both Γ_Δ and the shape of the cross section. This is illustrated by experimental data, shown in Fig. 8, on the photoabsorption cross sections of 1d2s-shell nuclei in the range from ^{16}O to calcium isotopes.

It has become obvious that 1p1h calculations are insufficient for reproducing the actual situation, and the space of possible excited configurations must be extended by taking states with more particles and holes into account (Fig. 9). These new configurations become relevant at the stage of the decay of the collective dipole state under the action of a 'friction' mechanism, which is realized, for example, due to the coupling of dipole oscillations to quadrupole surface vibrations. Back in 1962, it was shown in [47] that some '1p1h + phonon' 2p2h states can substantially affect the GDR width and structure.

In the framework of the collective model, this was considered in [48, 49], where the coupling of dipole oscillations and quadrupole vibrations was taken into account in spherical nuclei. In [50], dipole states were considered in the framework of the particle-hole approach, but surface vibrations were still described within the collective model, with up to six quadrupole phonons taken into account. The data for ^{60}Ni given in [50] are compared in Fig. 10 with the results of the experiment in [51]. We can see that going beyond the 1p1h approach due to the coupling of dipole and quadrupole degrees of freedom, i.e., passing from the basis of 1p1h configurations to the basis of 2p2h configurations (the quadrupole surface excitations, just as the dipole ones, correspond to collectivized 1p1h-states in the microscopic picture), leads to significant fragmentation and the spread of the dipole strength of a coherent 1p1h excitation. The GDR shape predicted by the theory is then in much better correspondence with the observed complicated structure of the reaction cross section.

Taking more complicated excitations beyond the 1p1h ones into account also allows gaining insight into the nature of photonucleon energy spectra. The process of consecutive increase in the number of particle-hole pairs in the excited nucleus is completed at the compound nucleus stage,

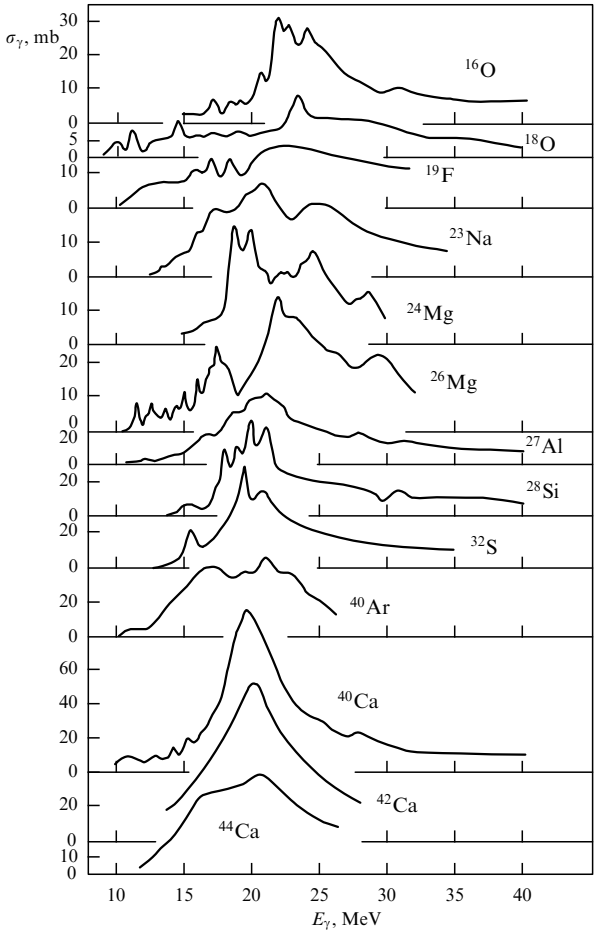

Figure 8. Experimental photoabsorption cross sections of 1d2s-shell nuclei [46].

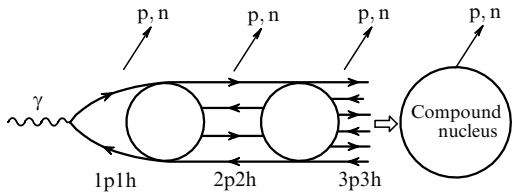

Figure 9. Process of the increase in the number of particle–hole pairs and emission of nucleons at different stages of GDR decay.

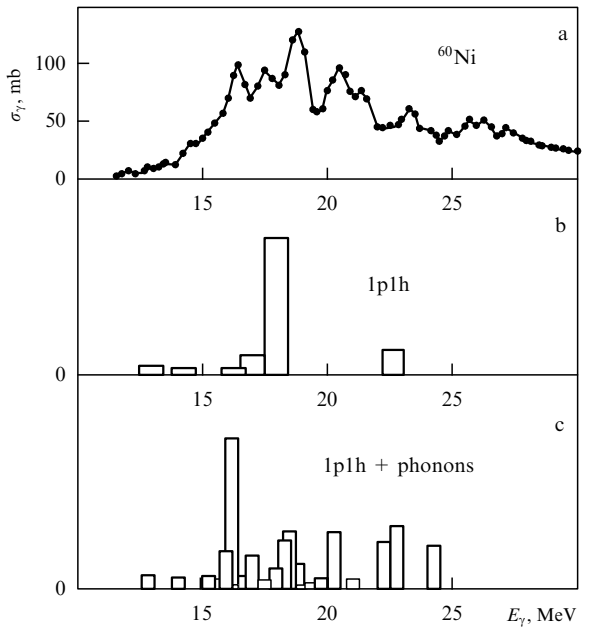

Figure 10. (a) Photoabsorption cross section for the ^{60}Ni nucleus obtained by adding the photoproton and photoneutron cross sections [51], and result of the calculation of the dipole strength (in relative units) (b) within the 1p1h approach and (c) with the coupling of 1p1h states to surface phonons taken into account [50].

(1p1h $\rightarrow$ 2p2h $\rightarrow$ 3p3h $\rightarrow \ldots \rightarrow$ compound nucleus), with the nucleus capable of emitting a nucleon at each step of this process. If the nucleons are emitted at the first step, the resultant spectrum is rather hard, as predicted by 1p1h calculations. If nucleons are emitted at the last step, an evaporative-type spectrum follows. These two spectra are limit idealizations of the real situation. A spectrum close to the observed one can be obtained if the emission of nucleons at all steps of the above process is taken into account. As the number of ph pairs increases, the emitted nucleons become less energetic, and their spectrum changes from a hard ('direct') to a softer ('evaporative') one.

In this way, about 10 years after the appearance of the particle-hole GDR model, it became obvious that a detailed description of GDR must involve not only 1p1h states but also 2p2h states at the very least. Theoreticians invested considerable effort into implementing this idea. Exactly taking all possible 2p2h configurations into account is impossible because of their huge density in the GDR range, up to 10^3-10^4 states per MeV in intermediate-mass and heavy nuclei. In the approach that was used instead, noncoherent 2p2h configurations were replaced by states of the '1p1h + phonon' type, as in [50], or of the 'phonon + phonon' type. Within that approach, rules can be justified for selecting such 2p2h configurations (including, first and foremost, phonons corresponding to collective excitations) that have the strongest effect on the GDR structure and width.

In [52], for example, the coupling of coherent 1p1h states to more complicated two-phonon states was for the first time taken into account within the quasiparticle-phonon model for heavy spherical nuclei, and in TFFS calculations [53, 54] that included the continuum and the standard set of residual forces, similar effects were investigated for intermediate-mass and heavy closed-shell nuclei. To bypass complications in applying the 1p1h + 2p2h approach that ensue even after the most important 2p2h states are selected, the effects of damping of dipole oscillations were taken into account phenomenologically in a number of cases [55].

The calculation difficulty increases very sharply as the configuration space is extended by including 2p2h, 3p3h, and more complicated configurations, and it is also quite difficult to even estimate the error. This limits the use of such an approach to magic nuclei and those close to them.

The existing microscopic calculations, with rare exceptions, do not reproduce exclusive characteristics, such as partial GDR decay channels, and become invalid in describing the GDR structure. This explains why there remains some interest in different semimicroscopic and phenomenological ways to describe GDR, e.g., in [56, 57].

Because the success of microscopic GDR calculations depends on the choice of the nucleon-nucleon interaction, it is useful to investigate GDR within an approach based on the energy density functional. In this approach, which works well, in particular, in describing neutron-excess isotopes [58–60], the mean field of the nucleus and the interaction in the particle–hole channel are determined self-consistently.

5. Problem of giant dipole resonance width and structure

To reliably identify the nature of the GDR width and structure and to understand the role of various configurations in their forming, we must turn to experimental studies. As has been shown experimentally, a decisive test for deciphering the configurational structure of GDR consists of identifying nucleon decay channels, especially those with a fixed populated state of the final nucleus. The desire to decipher this structure has stimulated progress in experimental methods for investigating photonuclear reactions. We note the most important stages reached along this path.

From the start of photonuclear investigations, attempts were made to create sources of monochromatic high-energy gamma quanta so as to bypass the difficulty in interpreting experiments with continuous bremsstrahlung photons. Such sources have been produced, and their use has led to the appearance of a large amount of data on GDR, which together with alternative results of numerous 'bremsstrahlung experiments' increased the overall reliability of experimental information. Three main methods for monochromatization have been proposed and developed: 'tagging' bremsstrahlung photons, Compton backscattering, and in-flight annihilation of fast positrons.

The method of tagged photons was first carried out using the Cornell University synchrotron, USA [61]. Later, this method was used at the University of Illinois betatron [62, 63] for measurements of the photon scattering cross section on ^{197}Au and ^{165}Ho nuclei in the GDR domain. This method is most efficient in combination with a continuous electron beam. Such a beam was obtained in Illinois on a superconducting linear accelerator [64] and used for measuring the ^{238}U photofission cross section in an energy range below the GDR energy. Subsequently, the method proved relevant in high-energy physics for generating monochromatic photons with an energy up to 1.5 GeV on continuous electron beams [65].

The use of Compton backscattering (a 180° scattering of low-energy monochromatic photons on a beam of ultrarelativistic electrons) to generate high-energy monochromatic

and polarized gamma quanta was proposed in [66, 67]. Because Compton backscattering of photons requires electrons with energies of several hundred MeV or more, this method was realized in laboratories involved in investigations in high-energy physics. Powerful lasers are used as the source of monochromatic photons. Recently, this method allowed obtaining photon beams suitable for studying GDR (see, e.g., [68]), and the corresponding experiments have started.

Among all the existing methods for monochromatization of gamma quanta, the method of in-flight annihilation of fast positrons [69] has been developed the most; in essence, this is the single method that has led to obtaining a large number of results. It was first realized in two nuclear centers: Saclay (France) [70] and Livermore (USA) [71]. The details of the realization of this method and the result can be found in review [72]. The moderate intensity of the annihilation photons limits their efficient use to a single type of experiment: measurements of the effective cross section of photoneutron reactions. The insufficiently high intensity of the annihilation radiation can be compensated in such experiments by a large mass of the investigated target and the use of high-efficiency (40–60%) neutron detectors. In 'annihilation experiments' on light nuclei, it has been possible to reveal the structure of the cross section for the increasing part of the GDR. Above the GDR maximum, the possibilities for resolving the structure with this method are reduced, because resonances in cross sections start being strongly excited by the 'bremsstrahlung,' i.e., continuous, part of the gamma spectrum that accompanies the annihilation peak. With the help of annihilation photons, valuable information has been obtained on cross sections of photoneutron reactions of different multiplicities: $(\gamma, 1n)$, $(\gamma, 2n)$, $(\gamma, 3n)$, and $(\gamma, 4n)$. A summary of the photoneutron cross sections obtained in 'annihilation experiments' is given in [73].

The use of bremsstrahlung gamma radiation remains one of the most important way to obtain information on GDR. The main advantage of that radiation is the high intensity of bremsstrahlung photons, several orders of magnitude greater than the intensity of monochromatic gamma beams. Returning to the annihilation method, it should more precisely be considered a method for producing quasimonochromatic photons, because the existence of a strong bremsstrahlung 'tail' requires performing two experiments, one with electrons and one with positrons, and then subtracting the results from one another. Such a difference procedure is also characteristic of bremsstrahlung experiments, but it is much more precise here because it does not require switching the accelerator from the positron acceleration regime over to the electron acceleration regime. In addition, systems have been constructed that ensure a high precision of stabilizing and controlling the upper edge of the bremsstrahlung spectrum and allow cyclically alternating it with the frequency of 50 Hz. The entire GDR range is then scanned within several seconds, and multiple repetitions of this cycle allow collecting the necessary statistics. This method for scanning the upper edge of the bremsstrahlung spectrum (proposed in [74]) significantly reduces the effect that the drift of the parameters of the devices registering the photonuclear reaction products has on the precision of the obtained data. In combination with well-developed methods for mapping the reaction yield into effective cross sections, the 'bremsstrahlung' photonuclear experiments remain quite relevant and in many cases are the only reliable source of information on the GDR parameters.

The experimental methods involving bremsstrahlung photons, as described above, have been developed and actively used by the photonuclear group of the Research Institute for Nuclear Physics (RINP) of Lomonosov Moscow State University since the early 1960s. The use of a betatron with an electron energy up to 35 MeV, overlapping the entire GDR range, together with high-efficiency detectors of neutrons, protons, and gamma quanta allowed deciphering the configurational GDR structure for nuclei with up to 60 nucleons and finding the quantitative contribution of semidirect nucleons to the decay of nuclei in that mass range. The role played by various factors in forming the GDR structure was clarified simultaneously. This progress was achieved due to shifting the center of gravity of photonuclear investigations from measurements of photoabsorption and photonucleon cross sections, which carry important but limited information on the GDR, to the characteristics of its decay, such as spectra of photonucleons, decay gamma quanta, and partial photonucleon cross sections with some levels in the final nuclei populated. The method of scanning the upper edge of the bremsstrahlung spectrum was used for the first time in measuring the spectra of decay products. The description of experimental methods used by the RINP photonuclear group and the procedures for extracting information and principles of its interpretation can be found in [46, 75–77].

In 1978, a data center for photonuclear experiments was created at RINP under the aegis of the International Atomic Energy Agency (IAEA) with the aim to organize and analyze a large amount of experimental information on photonuclear reactions (up to 100 publications per year) [78]. This data center, which became part of a network of international centers for nuclear data, contains the most complete information on the published photonuclear experiments [79], evaluates their reliability, and in some cases corrects them by applying a set of criteria [80]. Photonuclear data are also available from databases [81, 82].

The existence of vast photonuclear data pertaining to characteristics of GDR decay allows solving numerous problems encountered in theoretical research. First of all, there is the problem of the GDR width. For a long time, it had been unclear what causes the large spread (from 4 to 20 MeV) of Γ_Δ for nuclei with similar mass numbers A and what underlies the difference, in that regard, between light, intermediate-mass, and heavy nuclei. This problem is closely related to the structure observed in photonuclear cross sections. We can single out three types of structure elements that can be present in σ_γ: wide (3–5 MeV) domains of concentration of electric-dipole E1 transitions, called the gross structure (the *gross structure* of GDR in heavy nonspherical nuclei comprises two wide split maxima); more narrow (0.5–2.0 MeV) domains of concentration, called the *intermediate structure*; and very narrow ($\approx 0.05-0.1$ MeV) domains called the *fine structure*. The task was to establish how these structures are formed and how they affect the magnitude of Γ_Δ. Currently, we can answer all these questions based on the many years of experimental and theoretical research.

As we have noted, there are two possibilities for a 1p1h excitation to decay. The first amounts to the nucleus emitting a nucleon that has undergone the transition to a free shell as a result of the absorption of an E1 photon by the nucleus. The probability of that decay, called semidirect, is characterized by the escape width $\Gamma^\uparrow$, and just this decay leads to the

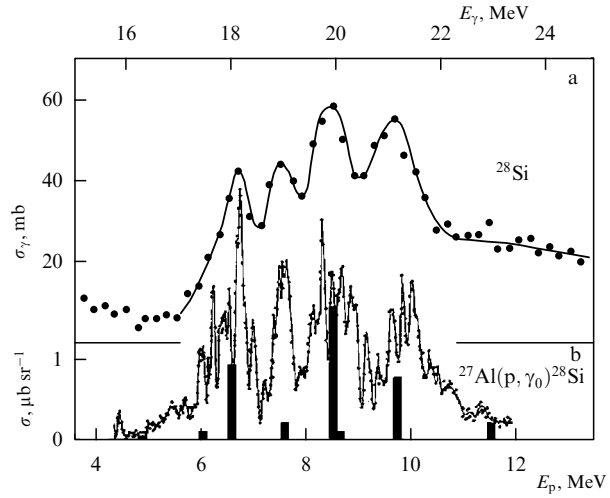

Figure 11. (a) Experimental photoabsorption cross section for the ^{28}Si nucleus in the GDR range [83]. (b) Experimental cross section of the reaction ^{27}Al(p, γ_0)^{28}Si in the GDR domain [84] and data of theoretical calculations [85] (columns).

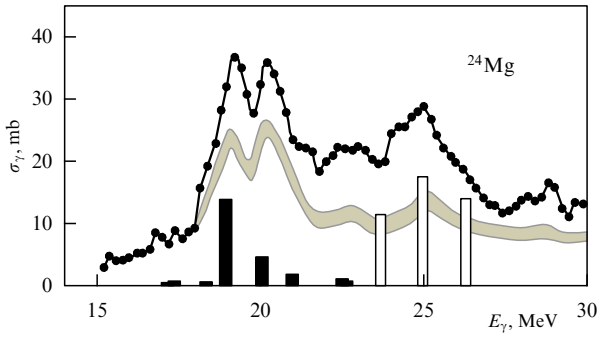

Figure 12. Photoabsorption cross sections for the ^{24}Mg nucleus obtained by adding the photoproton and photoneutron cross sections [86], and the semidirect component of this cross section (shaded strip). Columns: data of the 1p1h calculation in [87]. Dark columns correspond to the joint contribution of the 1d2s → 1f2p and $1p_{1/2}$ → 1d2s transitions; light columns, to $1p_{3/2}$ → 1d2s transitions.

appearance of the intermediate structure in photonuclear cross sections of light nuclei. We note that direct decay is not attended by the formation of GDR when the nucleon, bypassing the stage of transition to a free shell, directly escapes from the nucleus; the probability of this process in GDR is low. The second version of the 1p1h excitation decay is the transfer of a part of the energy of this excitation to another nucleon, i.e., the formation of one more 1p1h pair in the nucleus, which together with the original pair forms a 2p2h excitation in the nucleus. The corresponding probability is characterized by the width $\Gamma^{\downarrow}$, and it is this process that leads to the appearance of the fine structure of photonuclear cross sections. Evidently, the particle–hole structure of the original E1 excitation can undergo a chain of increasingly complex variations, 2p2h → 3p3h → ... → compound nucleus (see Fig. 9).

We can see from Fig. 11 how the intermediate and fine structures manifest themselves in the GDR of the ^{28}Si nucleus. The resolution of the photonuclear experiment does not allow us to 'see' the fine-structure resonances, but the intermediate-structure resonances are quite distinct (Fig. 11a). At the same time, fine-structure resonances can be seen in the (p, γ_0) inverse photonuclear reaction, the energy resolution of such reactions being much higher (Fig. 11b [84]). We can clearly see how these narrow resonances appear on the background of wider resonances of the intermediate structure. Vertical columns in Fig. 11b represent the data of 1p1h calculations in a multiparticle shell model [85]. Direct decay occurs in the time of $10^{-23}-10^{-22}$ s and semidirect, in 10^{-21} s, the so-called pre-equilibrium (2p2h, 3p3h) stage is reached in 10^{-20} s, and, finally, the compound nucleus stage (the setting in of statistical equilibrium), in $10^{-19}-10^{-18}$ s.

Experimental investigations of partial GDR decay channels by the method of spectral measurements of photonucleons (primarily photoprotons) and gamma quanta releasing the excitation of the final nuclei after the emission of a photonucleon from the nucleus have allowed clarifying the configurational structure of GDR in nuclei with up to 60 nucleons, with the role of the semidirect decay mechanism determined. This required using spectroscopy information on the hole (1h) levels in the final nuclei relative to the target nucleus obtained in independent reactions with a single-nucleon transfer. The population of such levels in the GDR decay implied that this decay occurred at the earliest (semidirect) stage: 1p1h → (nucleon emission) → 1h. Conversely, if the populated level had a more complicated nature, this was preceded by a later stage of the GDR decay: 2p2h, 3p3h, ... → (nucleon emission) → 1p2h, 2p3h, ... Identifying the populated 'hole' in the semidirect decay uniquely fixed the shell configuration of the original excited state. These investigations involved the entire volume of nuclear data available worldwide on partial GDR decay channels. For example, for 1d2s-shell nuclei ($A = 16-40$), more than 300 partial cross sections were used, and for 1f2p-shell nuclei with A in the range 40–60, about 100 partial cross sections were used. The investigations resulted in deciphering the GDR shell structure and determining the role of the semidirect decay mechanism for nuclei with up to 60 nucleons.

As an example, in Fig. 12 we show the experimental photoabsorption cross section on the ^{24}Mg nucleus, obtained by summing photonucleon cross sections; the part of the cross section that is formed due to the semidirect GDR decay mechanism is also shown. As experimental analysis shows, below 23 MeV the cross section is primarily formed by transitions from the outer shell: 1d2s → 1f2p, and above 23 MeV, by transitions from the inner shell: 1p → 1d2s. The same conclusions follow from theoretical calculations. This means that the phenomenon called configurational splitting of the GDR occurs [46]. It is characteristic of nuclei with up to 60 nucleons. The configurational splitting magnitude decreases as the mass number increases and attains a maximum of 10–15 MeV for 1p-shell nuclei. In 1d2s-shell nuclei, it decreases to 5–10 MeV and can be traced for nuclei with mass numbers down to the A of nickel. This effect is the main factor behind the formation of the gross structure of light nuclei.

The experimental investigations described above also allowed clarifying the quantitative role of the semidirect GDR decay mechanism in nuclei of the relevant mass range. It turns out that, in 1p-shell nuclei, the GDR decay is virtually entirely determined by this mechanism. In 1d2s-shell nuclei, the semidirect mechanism is also dominant, being responsible for 60–70% of decays in the domain of the GDR maximum, or even more in the photoneutron channel. As the mass

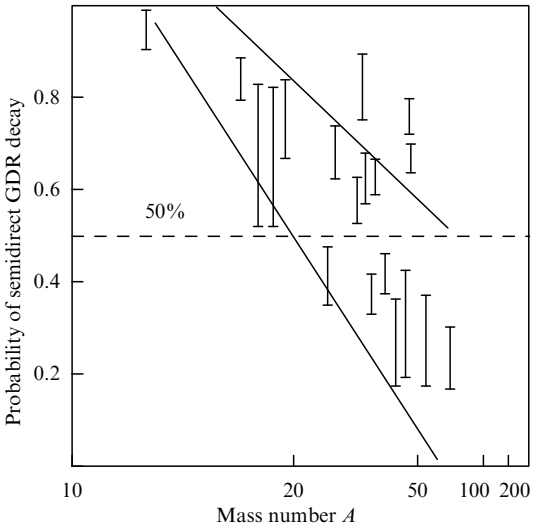

Figure 13. Probability of semidirect GDR decay as a function of the mass number A based on the analysis of experimental data.

number A increases, the probability of semidirect GDR decay rapidly decreases, which is explained by a rapid increase in the density of the 2p2h dipole states into which the original 1p1h excitation can decay. In heavy nuclei with $A \approx 200$, the semidirect decay is responsible for only about 10% of the total GDR decay probability. The tendency of the semidirect GDR decay probability to decrease as the mass number increases is illustrated in Fig. 13.

Experimental investigations, together with theoretical research, established the role of a variety of factors operating in forming the GDR structure and width in nuclei with different numbers of nucleons. Self-conjugate and light 1p- and 1d2s-shell nuclei (^{12}C, ^{16}O, ^{28}Si, and ^{40}Ca), as well as spherical nuclei with the magic numbers of neutrons and (or) protons ($N = 50$, $Z = 50$, $N = 82$, $Z = 82$, and $N = 126$), or nuclei close to these, are the simplest from the standpoint of the shape and structure of photoabsorption cross sections and the understanding of how this shape and this structure form. In experiments with moderate energy resolution, the GDR for such nuclei is represented by a resonance of the width $\Gamma_0 \approx 4-5$ MeV, which we call 'magic.' We cannot speak of a pronounced gross structure of such nuclei. In experiments with high energy resolution in light nuclei, the intermediate structure transpires. Resonances of this intermediate structure have the width of 0.5–2.0 MeV and are primarily caused by the semidirect decay of the original dipole 1p1h states. The GDR width of 4–5 MeV in these light nuclei is largely due to the Landau damping — energy spread of E1 transitions of nucleons from one (outer) shell.

In heavy spherical nuclei, the intermediate structure disappears as a result of the effect of friction caused by the decay of the original collectivized 1p1h states into type-2p2h states, whose number can reach $10^3 - 10^4$ in a 1-MeV interval. In theoretical calculations, this form of friction, as we have noted, is taken into account by the decay of the original collectivized 1p1h states into type-2p2h states, which are the most important as regards the formation of the GDR width and structure and which occur due to the coupling of proton-neutron E1 oscillations to the nucleus surface and have the configuration of two interacting phonons (one of which is a dipole and the other a quadrupole). If such friction were absent, most of the dipole strength of GDR in heavy spherical nuclei under the action of the Brown–Bolsterly collectivization mechanism would be concentrated in one coherent 1p1h state of a small proper width $\Gamma^{\uparrow} \approx 0.2-0.6$ MeV, determined by the emission of semidirect nucleons (primarily neutrons) from that state into the continuum. The observed GDR width in such nuclei quoted above, 4–5 MeV, is due to the width of the domain of spread of the original dipole (1p1h) states over the most intense two-phonon (2p2h) states.

The width Γ_{Δ} of all spherical nuclei and nuclei with filled nucleon levels is described by the relation $\Gamma_{\Delta} \approx \Gamma_0$; in light nuclei, the main contribution to Γ_{Δ} is made by $\Gamma^{\uparrow}$ and Landau damping, and in heavy nuclei, by $\Gamma^{\downarrow}$. A decisive role in this tendency observed in passing from light to heavy nuclei is played by the rapid increase in the density of dipole 2p2h states, into which the original 1p1h excitations can decay.

In nuclei with nonfilled nucleon shells and in nonspherical nuclei, an important role in the formation of Γ_{Δ} is played by effects due to the gross structure of GDR. There are three such effects:

(1) splitting in the energy of E1 transitions from different (typically two) shells (configurational splitting);

(2) GDR splitting related to properties of the isospin quantum number (isospin splitting [88, 89]);

(3) GDR splitting related to the deformation of the nucleus in the ground state.

For nonmagic light nuclei with a mass number up to $A \approx 40$, configurational splitting is the main factor behind the increase in the GDR width Γ_{Δ} compared with the 4–5-MeV value. The role of this form of GDR splitting, even though it was observed in nuclei with A up to 60, decreases as A increases, because the shells are drawn closer to each other, and it can be disregarded for intermediate-mass and heavy nuclei.

Isospin GDR splitting occurs in non-self-conjugate nuclei with $N \neq Z$. In these nuclei, two energy-separated GDR branches occur, with the isospins $T_< = T_0$ and $T_> = T_0 + 1$, where $T_0 = (N - Z)/2$ is the isospin of the ground state of the nucleus, with the $T_>$ branch being higher in energy. In heavy nuclei, the role of isospin splitting in forming the GDR width is insignificant, because the probability of the excitation of the $T_>$ branch is low in these nuclei, despite a splitting magnitude that can reach 12 MeV. The isospin GDR splitting manifests itself in nuclei with up to 50–60 nucleons, because the probabilities of the excitation of isospin components in such nuclei are comparable for a sufficiently large splitting (up to 5–10 MeV).

The most conspicuous manifestation of the isospin GDR splitting is the shift, as the mass number increases, of the photoproton cross section maximum toward higher energies compared with the photoneutron cross section maximum (Fig. 14). This shift is a consequence of the fact that the GDR branch with the isospin $T_>$ decays primarily via the proton channel: $T_> \xrightarrow{\text{p}} T_0 + 1/2$ and $T_0 + 3/2$ (the $T_< \xrightarrow{\text{p}} T_0 + 1/2$ branch is suppressed by the Coulomb barrier due to lower proton energies). At the same time, the $T_<$ branch decays primarily via the neutron channel as a result of a higher probability of excitation of that branch in heavy nuclei than of $T_>$ branch excitation (Fig. 15). The isospin splitting magnitude increases as the neutron excess $(N-Z)$ increases.

In Figure 16, we show a manifestation of the isospin structure in the experimental photoabsorption cross sections for carbon isotopes. In the self-conjugate nucleus ^{12}C, E1

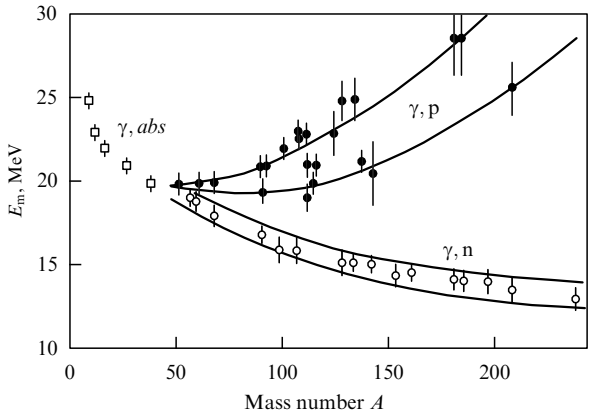

Figure 14. Energies of the cross section maxima for the photoproton reaction (dots) and the photoneutron reaction (circles) as functions of A. For $A < 50$, the maxima of these cross sections practically coincide.

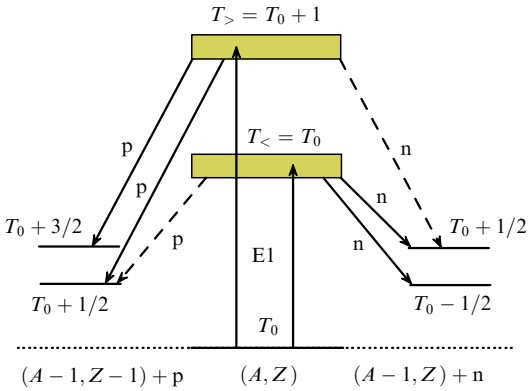

Figure 15. Isospin of GDR excitation and decay in the proton and neutron channels. Solid arrows show the main nucleon branches of the decay in heavy nuclei.

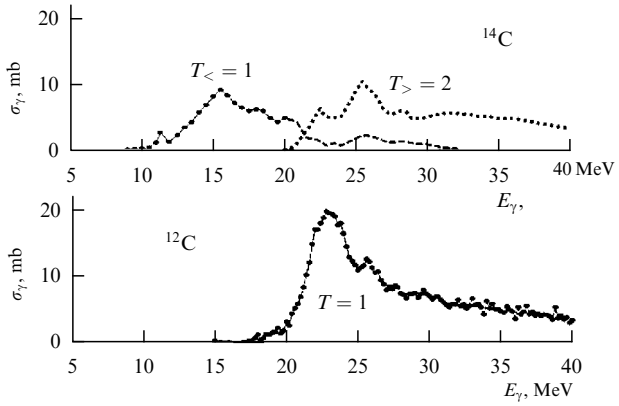

Figure 16. Isospin structure of photoabsorption cross sections in ^{12}C and ^{14}C nuclei. For the ^{14}C nucleus, the experimental cross section is decomposed into isospin components in accordance with the analysis in [90].

excitations are possible only with the isospin $T_> = 1$, but in ^{14}C, E1 excitations with both $T_< = 1$ and $T_> = 2$ are possible. These components in ^{14}C are energy-separated by about 10 MeV and have comparable excitation probabilities.

Because most light nuclei are non-self-conjugate and nonspherical, the shape of their photoabsorption cross sections must be strongly affected by all three of the above factors responsible for the gross structure of GDR. An appropriate question to ask is about the relative role of these factors for the selected group of nuclei. We note, first, that because only the $T_<$ branch contributes to the E1 transitions of nucleons from outer shells, the energy ranges hosting the isospin and configurational splittings overlap. As regards the nonsphericity of the nuclei, there is no direct correlation between the GDR width and the quadrupole deformation parameter for nuclei with $A < 40$. The deformation affects the shell structure of the nucleus, rearranging the shells and changing the separation between them. Because the configurational GDR splitting reflects the shell structure of light nuclei, the nonsphericity of the nucleus is in fact automatically taken into account by that effect.

We now discuss nuclei with mass numbers from 40 to 120. The GDR widths in nuclei in this range are on average much lower than in light nuclei. Immediately after the calcium isotopes, they reach the maximum values of 10–11 MeV in the considered range of mass numbers, and for $A > 80$ nowhere exceed 8.5 MeV. Because in intermediate-mass and heavy nuclei the configurational and isospin splittings have no significant effect on the GDR width and the spread of 1p1h transitions from one shell and because the values of $\Gamma^\uparrow$ are not large, the main factors contributing to the increase in the GDR width over 4–5 MeV are only the decay width $\Gamma^\downarrow$ of the original states into states of a more complicated nature (2p2h, 3p3h, ...) and the nonsphericity of the nucleus ground state (the Danos–Okamoto effect). These factors are analyzed in [91] with the use of the entire volume of data on photoabsorption cross sections and the nonsphericity degree of nuclei available worldwide. It turns out that, for the nuclei under consideration, the correlation between Γ_Δ and the modulus of the quadrupole deformation parameter $|\delta|$ is either unessential or totally absent, which eliminates the Danos–Okamoto effect as the main factor responsible for GDR broadening in the chosen mass range. Most nuclei with $A = 40-120$ classify as soft vibrational nuclei, and many of them have a nearly spherical shape. In such nuclei, the GDR must be broadened due to the coupling of E1 oscillations to the nucleus surface oscillations, primarily quadrupole ones, which amounts to the dipole–quadrupole friction discussed above. Taking this coupling into account leads to a decay of the original dipole 1p1h excitations into excitations of a more complicated nature of the '1p1h + phonons' type, realized in terms of the GDR cross section shape via the intermediate structure, and in terms of the GDR width via the $\Gamma^\downarrow$ component.

To take the dipole–quadrupole friction into account in the nuclei under consideration, it suffices to use the dynamical collective model [48, 49] or the model of collective correlations [50]. The dipole–quadrupole interaction leads to the splitting of the collective E1 excitation into a number of transitions whose number and energy spread become greater as the dipole-quadrupole friction gets stronger. It is the resultant spread of E1 transitions that determines the GDR broadening in nonmagic vibrational nuclei. A detailed comparison of experimental and theoretical data [91] shows that in the mass number range $A = 40-120$ the dipole-quadrupole friction is the main factor behind the increase in the GDR width compared with the magic one (4–5 MeV). In that range of mass numbers, the GDR width due to this friction increases by 3–5 MeV on average.

In the range $A > 120$, where nuclei with higher static deformations cluster, the correlation between Γ_Δ and $|\delta|$ is

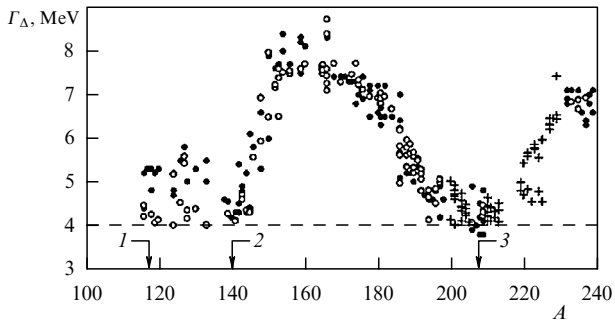

Figure 17. GDR widths of $A > 117$ nuclei [91]. Dark symbols: data from photonuclear experiments, light symbols and crosses: values extracted from the known quadrupole deformation parameters. Dotted line corresponds to the GDR width in magic nuclei. Arrows show the domains of magic nuclei: *1* — $Z = 50$; *2* — $N = 82$; *3* — $Z = 82$; $N = 126$.

obvious. For those nuclei that have a stronger quadrupole deformation ($|\delta| > 0.20$), the GDR acquires a gross structure in the form of two maxima, as in ^{165}Ho (see Fig. 2) and ^{154}Sm (see Fig. 4). In the absence of other factors that have a substantial impact on the gross structure of the GDR, its general shape in nonspherical axial nuclei can be represented as a superposition of two 'spherical' resonances with $\Gamma_0 =$ 4–5 MeV, separated in energy by $\Delta E \approx 75A^{-1/3}|\delta|$ MeV (see Eqn (4)). The GDR width in such nuclei must increase to $\Gamma_\Delta = \Gamma_0 + \Delta\Gamma$, where $\Delta\Gamma$ increases as ΔE increases, and if $\Delta\Gamma$ is proportional to ΔE, then it must also be proportional to $|\delta|$. Thus, as a consequence of the Danos–Okamoto effect, a correlation must be observed between the modulus of the quadrupole deformation parameter δ and the GDR width.

The use of all the currently available information on the GDR shape and the quadrupole deformation parameters for nuclei with $Z \geqslant 50$ allows investigating the problem of the effect that the quadrupole deformation has on the GDR characteristics with the maximal accessible precision and, in particular, answering the question of whether the nonsphericity is essentially the unique factor of GDR broadening in heavy nuclei and how strong the correlation is between GDR broadening and the magnitude of the deformation parameter.

The degree of this correlation is illustrated in Fig. 17, where for nuclei in the range $A > 117$ we show the widths of experimental photonuclear cross sections (dark symbols) and the GDR widths calculated from the value of $|\delta|$ by the relation $\Gamma_\Delta = \Gamma_0 + \Delta\Gamma$, where $\Gamma_0 = 4$ MeV and $\Delta\Gamma =$ $11|\delta|$ MeV (light symbols). Within the spread of the width values, the data of both types coincide in the entire range of mass numbers $140 < A < 240$. The degree of correlation is so high that there is no doubt that just the Danos–Okamoto effect (directly following from Migdal's concept) is responsible for the GDR broadening in nuclei with $A > 120-130$. The values of $\Delta\Gamma$ and $|\delta|$ to be compared are minimal in magic nuclei with $Z = 50$, $N = 82$ and $Z = 82$, $N = 126$ and reach maximum values at the midpoint between these domains. We note that the proportionality coefficient between $|\delta|$ and $\Delta\Gamma$, as follows from formula (4), differs by only 10–15% from the number 11 obtained by a fit to experimental data.

The level of correlation of the data to be compared allows predicting the GDR widths in the mass number range $A = 200-230$, where photonuclear cross sections have not been measured due to the absence of stable isotopes, but data on the electric quadrupole moments (and, hence, on the deformation parameters) are available. Suitable for such a prediction, naturally, is the relation $\Gamma_\Delta = (4 + 11|\delta|)$ MeV. The obtained values are shown with crosses in Fig. 17. With these additional values, Fig. 17 presents the pattern of the GDR width behavior depending on the mass number for all of the heavy nuclei.

The Danos–Okamoto effect shows that a heavy nucleus that has absorbed a high-energy photon preserves its deformation during the GDR lifetime ($10^{-19}-10^{-18}$ s). Why is it that the original shape of the nucleus not only avoids destruction during that sufficiently long time, by nuclear standards (up to 10^4 nuclear times), but also remains largely unperturbed in nuclei with the excitation energy ≈ 15 MeV? We can list the following factors conducive to the preservation of the deformation degree by the nucleus. The GDR formation involves nucleons of outer nuclear shells. Hence, in a heavy nucleus, the nucleon core lying below the outer shells is not affected by the photosplitting process in general. In a heavy nucleus, this core makes up the main part of the nucleus and it is its polarization by long-range residual forces that is largely related to the nonsphericity of the nucleus in the ground state. Deformation of the nucleus shape is also determined by nucleons near the Fermi surface, which are affected by E1 excitations. But, under such excitations, there is a high probability that the one-particle states with large orbital moments, which make the nucleus unstable to changes in the deformation, are not populated.

The picture is different with light nuclei. All the shells of 1p nuclei and two out of three shells of 1d2s nuclei are involved in the photosplitting process, and it is therefore natural to expect at least a partial loss by the nucleus of its original (static) deformation. The degree to which the faster (semidirect, with the time $\approx 10^{-21}$ s) GDR decay of a light nucleus helps preserve the deformation remains to be established.

GDR is a 'response' of the nucleus to the time-dependent external electric 'dipole' field. External fields, however, can have different multipole patterns and different natures. Accordingly, the problem arises of a collective response of the nucleus to these fields, and the ensuing problem of other resonances. These so-called giant multipole resonances (GMRs), distinct from GDR, were discovered in the 1970s in the reactions (e, e'), (α, α'), (p, p'), (p, n), (π^+, π^0), $(^3\mathrm{He}, t)$, (μ, ν_μ) and so on. The new giant resonances have common features with GDR: the concentration in a relatively narrow energy range several MeV in width and the manifest signatures of collectivity. The study of these resonance profits from the theoretical approaches developed in GDR investigations. Information on the discovered GMRs and the relevant references can be found in reviews [32, 92–94].

6. New forms of giant dipole resonance

Notably, studies of GDR proper have revealed some new nontrivial features. The 'classical' GDR is an excitation of a nucleus in the ground state. Almost four decades after the appearance of Migdal's pivotal work, GDRs were found that are constructed on individual excited nuclear states [32, 92–94], in reactions of radiation proton capture, in Coulomb excitation in heavy-ion collisions, in double charge exchange (π^+, π^-), and others. These excitations can be viewed, for example, as two-phonon GDR-type 2p2h states, constructed over one of the ph states. Excitations are observed that

correspond to double GDR (GDR + GDR), GDR over a giant quadrupole resonance (GDR + GQR), and GDR over an isobar-analogue state (GDR + IAS). The energies of these two-phonon states coincide with the total energy of one-phonon states, and in the course of their decay each phonon decays independently of the other.

Another new avenue in the physics of GDR amounts to its observation and investigation in heated nuclei. In such nuclei, with the temperature given by, say, 1–2 MeV, due to the increased probability of pairwise collisions, the motion of nucleons becomes much more chaotic, and it is not obvious a priori whether the collective motion of nucleons would be sufficiently stable to withstand the thermal chaos. Therefore, the discovery of dipole oscillations in strongly excited nuclei (with the excitation energy ≈ 100 MeV) was quite a notable event (the relevant references and their analysis are available in reviews [32, 95]). The data were derived from an analysis of the spectra of high-energy photons emitted by the compound nuclei formed in heavy-ion collisions. These data lead to the following conclusions: 1) the existence of dipole oscillations is a universal property of heated nuclei; 2) the frequency of these oscillations, i.e., the energy at the GDR maximum, differs little from the GDR frequency in cold nuclei; 3) GDR in a heated nucleus corresponds to a well-collectivized state; 4) the GDR width in such nuclei exceeds its width in cold nuclei and increases as the excitation energy (temperature) increases, attaining saturation ($\Gamma \approx 13$ MeV) at $E^* \approx 100$ MeV.

Analysis shows that the contribution of 2p2h states to the GDR width in heated nuclei does not increase significantly compared with cold nuclei. It is assumed that the increase in width Γ is primarily determined by thermodynamic fluctuations of the deformation acquired by the originally spherical nucleus under heating.

An unusual phenomenon related to GDR in heated nuclei is as follows. In the fusion of two heavy ions, a state with a large number of particles and holes is produced. On the other hand, GDR corresponds to particle-hole oscillations. This results in an unusual situation: in cold nuclei, the pre-equilibrium dynamics start with ph-states and develop in the direction of multiparticle configurations, whereas in hot nuclei, the processes run in the reverse direction.

7. Giant dipole resonance analogues in nonnuclear microsystems

Remarkably, several decades after the discovery of nuclear GDR, its analogues were found in multiparticle nonnuclear systems such as atoms [96–99], metallic clusters (MCs) [100–102], and fullerenes [103, 104]. In all these objects, the giant resonance has the shape of a strong and wide peak corresponding to a collective excitation of many particles. This resonance peak exhausts most of the dipole oscillator strength.

Atomic resonances were first observed in atoms of noble gases and lanthanides. In [105], a similarity between atomic collective excitations and nuclear GDR was noted for the first time. In Fig. 18, we show the dependence of the electron yield of metallic lanthanum on the energy of a synchrotron radiation photon. The observed wide resonance is due to the electron transitions $4d^{10} \rightarrow 4d^9 4f^1$. Hartree–Fock calculations are indicative of collectivization of excitations, leading to a degeneration of the one-particle spectrum and a shift of the dipole oscillator strength toward higher energies.

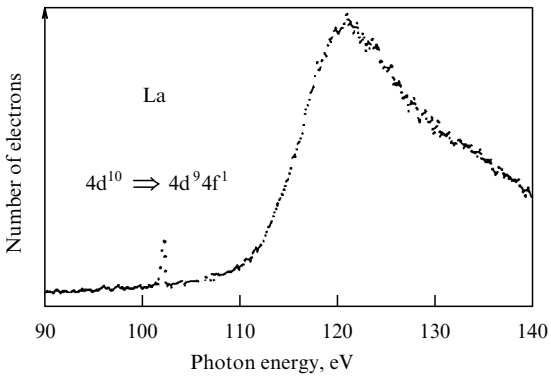

Figure 18. Electron yield from metallic lanthanum under the action of synchrotron radiation [106].

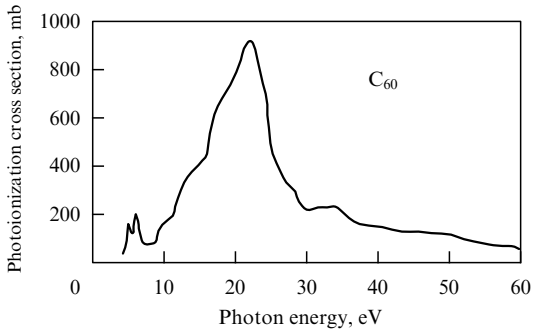

Figure 19. Total photoabsorption (below 25 eV) and photoionization (above 25 eV) cross sections for fullerene C_{60} according to the data from the experiment in [107].

Fullerenes and MCs host collective, primarily dipole, excitations of delocalized electrons (free electron gas) that occur under the action of an external electromagnetic field and are called *plasmons*. In Fig. 19, we show photoabsorption and photoionization cross sections for the C_{60} fullerene, which have a characteristic resonance shape.

The closest analogy between GDR and dipole excitations at the level of atoms and molecules is known for MCs — bound systems of atoms of some metals with spatially delocalized valence (conducting) electrons located in the field of positively charged ions. Similarly to the nucleus, an MC is a system where almost free electrons move in the mean field created by ions. The MC radius, as in the case of a nucleus, is proportional to the cubic root of the number of these particles, $N^{1/3}$, where N is the number of atoms in a cluster. Radial densities of valence electrons, similarly to nucleons in a nucleus, obey the Fermi distribution. It has been shown that shells exist in MCs and have the same magic numbers as in atomic nuclei and atoms. MCs are known with N up to 20,000. They can therefore be regarded as intermediate objects between atoms and solid bodies. There are two more features bringing MCs closer to atomic nuclei: the importance of surface effects and the possibility of shape deformation in both cases. It is therefore not accidental that, despite the different nature of interaction forces, theoretical methods developed in nuclear physics turn out to be applicable in the physics of MCs. More details on MCs can be found in review [108].

In Figure 20, we show giant resonances in fragmentation cross sections of small single-ionized MCs of silver. The cross

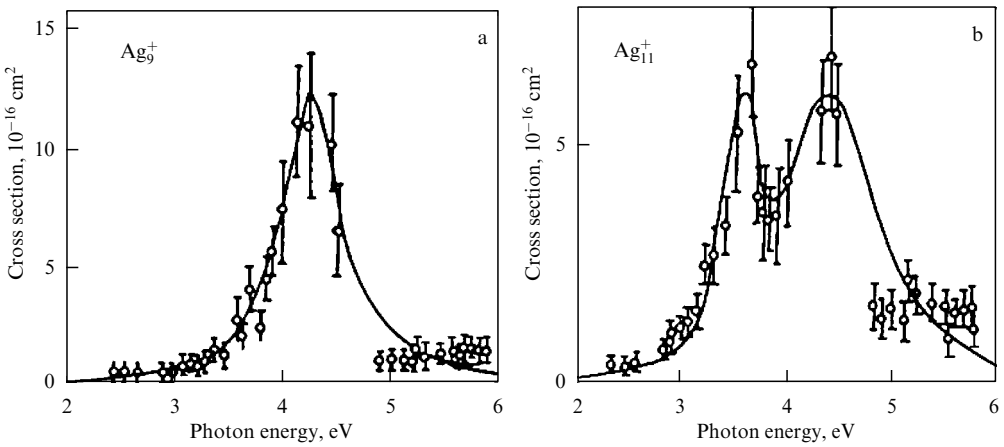

Figure 20. Giant resonances in fragmentation cross sections for single-ionized clusters of silver with (a) a filled shell ($N = 8$) and (b) a nonfilled shell ($N = 10$) [102].

section in Fig. 20a, which has the shape of a regular resonance, relates to a magic MC with 8 valence electrons. This cluster has closed shells and is therefore spherical. As expected, the cross section for it has the shape of a single resonance. The cross section in Fig. 20b relates to an MC with a nonclosed outer shell (with 10 valence electrons) and is split as a result of deformation. Thus, MCs also exhibit an effect similar to the Danos–Okamoto effect.

The mechanism of giant resonance broadening in small clusters is known from the physics of GDR: the coupling to quadrupole surface vibrations. Thermal fluctuations of the shape of small clusters are also an essential factor in resonance line broadening [109]. The same mechanism explains the broadening of collective resonances in heated nuclei.

A comparative analysis of giant resonances in nuclei, atoms, atomic clusters, fullerenes, and condensed media is available in [110]; the upshot is that the existence of giant resonances is independent of the nature of particles and interaction forces. Under certain conditions (the form of the mean field, the steepness of the boundary of the effective potential, the number of particles), such resonances are inevitable.

8. Conclusions

In Migdal's pivotal study [1] predicting GDR, the concept of quantum collective excitation modes was actually introduced into nuclear physics for the first time. GDR has been under study for three quarters of a century. In that period, a huge number of experimental and theoretical investigations have been conducted, and we can presently assume that the physics of this unique nuclear phenomenon is understood sufficiently well. GDR is inherent in all nuclei, and it remains in a class of its own among other nuclear phenomena in terms of how conspicuous and universal its manifestations are. Adopting an energy-wise division of nuclear physics, to low energies (nuclear spectroscopy at energies below the nucleon binding energy) and to high energies (in excess of that energy), we can say that the essential information on high-energy nuclear dynamics was in fact derived from investigations directly related to or motivated by GDR. It suffices to note that the entirety of the physics of GMRs of atomic nuclei emerged from the physics of GDR.

Giant resonance has been studied experimentally for most stable atomic nuclei, and we have a rich taxonomy of data available to the scientific community worldwide and covering the entire periodic system of elements. Analyses of these vast data and attempts to interpret them within various theoretical approaches have resulted in a breakthrough in the understanding of the physics of nuclear excitations with energies of 10–100 MeV. Moreover, direct links have been revealed relating this physics to the properties of ground and low-lying nuclear states, which yielded a unified picture of the principal nuclear phenomena.

Some of the most substantial and demonstrative achievements in nuclear physics directly related to GDR were the emergence of the multiparticle shell model and the theory of finite Fermi systems, which have allowed collective nuclear excitations to be explained in a distinctly microscopic approach.

It is remarkable that the physics of giant resonances has also been given a 'pass' outside nuclear physics. The electric GDR is observed in nonnuclear system such as atoms, MCs, and fullerenes. Moreover, the main theoretical approaches used in describing giant resonances in these systems are directly inherited from nuclear physics.

Giant dipole resonance has turned out to be very rich in its physical contents, and the initiation of studies in this new and extremely fruitful avenue in nuclear physics and several related areas is rightfully credited to Arkady Beinusovich Migdal.

References

1. Migdal A *J. Phys. USSR* **8** 331 (1944); Migdal A B *Zh. Eksp. Teor. Fiz.* **15** 81 (1945)
2. Bothe W, Gentner W *Z. Phys.* **106** 236 (1937)
3. Baldwin G C, Klaiber G S *Phys. Rev.* **71** 3 (1947); *Phys. Rev.* **73** 1156 (1948)
4. Goldhaber M, Teller E *Phys. Rev.* **74** 1046 (1948)
5. Steinwedel H, Jensen J H D *Z. Naturforsch. A* **5** 413 (1950)
6. Danos M *Nucl. Phys.* **5** 23 (1958)
7. Okamoto K *Phys. Rev.* **110** 143 (1958)
8. Carlos P et al. *Nucl. Phys. A* **225** 171 (1974)
9. Migdal A B *Nuclear Theory*; *the Quasiparticle Method* (New York: W.A. Benjamin, 1968); Translated from Russian: *Metod Kvazichastits v Teorii Yadra* (Moscow: Nauka, 1967)
10. Migdal A B *Theory of Finite Fermi Systems, and Applications to Atomic Nuclei* (New York: Interscience Publ., 1967); Translated from Russian, 1st ed.: *Teoriya Konechnykh Fermi-Sistem i Svoistva Atomnykh Yader* (Moscow: Nauka, 1983)
11. Migdal A B, Lushnikov A A, Zaretsky D F *Nucl. Phys.* **66** 193 (1965)

12. Lushnikov A A, Urin M G *Sov. J. Nucl. Phys.* **66** 311 (1965); *Yad. Fiz.* **1** 436 (1965)
13. Levinger J S, Bethe H A *Phys. Rev.* **78** 115 (1950)
14. Bogdankevich O V, Nikolaev F A *Methods in Bremsstrahlung Research* (New York: Academic Press, 1966); Translated from Russian: *Rabota s Puchkom Tormoznogo Izlucheniya* (Moscow: Atomizdat, 1964)
15. Bergere R, in *Photonuclear Reactions I: Intern. School on Electro- and Photonuclear Reactions, Erice, Italy, 1976* (Lecture Notes in Physics, Vol. 61, Eds S Costa, C Schaerf) (Berlin: Springer-Verlag, 1977) p. 1
16. Ishkhanov B S, Kapitonov I M *Vzaimodeistvie Elektromagnitnogo Izlucheniya s Atomnymi Yadrami* (Moscow: Izd. Mosk. Univ., 1979)
17. Goldemberg J, Katz L *Phys. Rev.* **89** 1300 (1953)
18. Penfold A S, Leiss J E *Phys. Rev.* **114** 1332 (1959)
19. Cook B C *Nucl. Instrum. Meth.* **24** 256 (1963)
20. Tikhonov A N *Dokl. Akad. Nauk SSSR* **151** 504 (1963)
21. Tikhonov A N et al. *Vestn. Mosk. Univ. Ser. Fiz. Astron.* **11** (2) 208 (1970)
22. Korotkova V A, Cherenkov P A, Chuvilo I V *Sov. Phys. Dokl.* **1** 77 (1956); *Dokl. Akad. Nauk SSSR* **106** 633 (1956)
23. Gavrilov B I, Lazareva L E *Sov. Phys. JETP* **3** 871 (1956); *Zh. Eksp. Teor. Fiz.* **30** 855 (1956)
24. Leikin E M, Osokina R M, Ratner B S *Dokl. Akad. Nauk SSSR* **102** 245 (1955); *Dokl. Akad. Nauk SSSR* **102** 493 (1955)
25. Osokina R M, Ratner B S *Sov. Phys. JETP* **5** 1 (1957); *Zh. Eksp. Teor. Fiz.* **32** 20 (1957)
26. Koch H W, Foote R S *Phys. Rev.* **91** 455 (1953)
27. Burgov N A et al. *Sov. Phys. JETP* **16** 50 (1963); *Zh. Eksp. Teor. Fiz.* **43** 70 (1062)
28. Dolbilkin B S et al. *JETP Lett.* **1** 148 (1965); *Pis'ma Zh. Eksp. Teor. Fiz.* **1** 47 (1965)
29. Dular J et al. *Nucl. Phys.* **14** 131 (1959)
30. Miklažič U et al. *Nucl. Phys.* **31** 570 (1962)
31. Danos M et al. *Phys. Usp.* **38** 1297 (1995); *Usp. Fiz. Nauk* **165** 1345 (1995)
32. Ishkhanov B S, Yudin N P, Eramzhyan R A *Phys. Part. Nucl.* **31** 149 (2000); *Fiz. Elem. Chast. At. Yad.* **31** 313 (2000)
33. Mayer M G, Jensen J H *Elementary Theory of Nuclear Shell Structure* (New York: Wiley, 1955)
34. Levinger J S *Nuclear Photo-Disintegration* (London: Oxford Univ. Press, 1960)
35. Wilkinson D H *Physica* **22** 1039 (1956)
36. Brink D M *Nucl. Phys.* **4** 215 (1957)
37. Elliot J P, Flowers B H *Proc. R. Soc. Lond.* **242** 57 (1957)
38. Neudachin V G, Shevchenko V G, Yudin N P *Sov. Phys. JETP* **12** 79 (1961); *Zh. Eksp. Teor. Fiz.* **39** 108 (1960)
39. Brown G E, Bolsterli M *Phys. Rev. Lett.* **3** 472 (1959)
40. Balashov V V, Shevchenko V G, Yudin N P *Sov. Phys. JETP* **14** 1371 (1962); *Zh. Eksp. Teor. Fiz.* **41** 1929 (1961)
41. Gillet V, Vinh Mau N *Nucl. Phys.* **54** 321 (1964)
42. Brown G E *Unified Theory of Nuclear Models* (Amsterdam: North-Holland Publ. Co., 1964); Translated from Russian: *Edinaya Teoriya Yadernykh Modelei i Sil* (Moscow: Atomizdat, 1970)
43. Buck B, Hill A D *Nucl. Phys. A* **95** 271 (1967)
44. Marangoni M, Sarius A M *Nucl. Phys. A* **132** 649 (1969)
45. Shlomo S, Bertsch G *Nucl. Phys. A* **243** 507 (1975)
46. Eramzhyan R A et al. *Phys. Rep.* **136** 229 (1986)
47. Balashov V V, Chernov V M *Sov. Phys. JETP* **16** 162 (1963); *Zh. Eksp. Teor. Fiz.* **43** 227 (1962)
48. Danos M, Greiner W *Phys. Rev.* **134** B284 (1964)
49. Huber M G et al. *Phys. Rev.* **155** 1073 (1967)
50. Drechsel D, Seaborn J B, Greiner W *Phys. Rev.* **162** 983 (1967)
51. Ishkhanov B S et al. *Sov. J. Nucl. Phys.* **11** 272 (1970); *Yad. Fiz.* **11** 485 (1970)
52. Soloviev V G, Stoyanov Ch, Vdovin A I *Nucl. Phys. A* **288** 376 (1977)
53. Kamerdzhiev S et al. *Nucl. Phys. A* **555** 90 (1993)
54. Kamerdzhiev S P, Tertychnyi G Ya, Tselyaev V I *Phys. Part. Nucl.* **28** 134 (1997); *Fiz. Elem. Chast. At. Yad.* **28** 333 (1997)
55. Rodin V A, Urin M H *Phys. Rev. C* **66** 064608 (2002)
56. Ishkhanov B S, Orlin V N *Phys. Part. Nucl.* **38** 232 (2007); *Fiz. Elem. Chast. At. Yad.* **38** 460 (2007)
57. Urin M H *Phys. Atom. Nucl.* **74** 1189 (2011); *Yad. Fiz.* **74** 1219 (2011)
58. Sapershtein E E et al. *JETP Lett.* **102** 417 (2015); *Pis'ma Zh. Eksp. Teor. Fiz.* **102** 475 (2015)
59. Borzov I N *Phys. Atom. Nucl.* **81** 680 (2018); *Yad. Fiz.* **81** 627 (2018)
60. Borzov I N, Tolokonnikov S V *Phys. Atom. Nucl.* **82** 560 (2019); *Yad. Fiz.* **82** 471 (2019)
61. Weil J M, McDaniel B D *Phys. Rev.* **92** 391 (1953)
62. O'Connell J S, Tipler P A, Axel P *Phys. Rev.* **126** 228 (1962)
63. Tipler P A et al. *Phys. Rev.* **129** 2096 (1963)
64. Dickey P A, Axel P *Phys. Rev. Lett.* **36** 501 (1975)
65. McGregor J C et al. *Eur. Phys. J. A* **37** 129 (2008)
66. Milburn R H *Phys. Rev. Lett.* **10** 75 (1963)
67. Arutyunyan F R, Gol'dman I I, Tumanyan V A *Sov. Phys. JETP* **18** 218 (1964); *Zh. Eksp. Teor. Fiz.* **45** 312 (1963)
68. Utsunomiya H, Hashimoto S, Miyamoto S *Nucl. Phys. News* **25** (3) 25 (2015)
69. Tzara C *CR Acad. Sci.* **245** 56 (1957)
70. Miller J, Schuhl C, Tzara C *Nucl. Phys.* **32** 236 (1962)
71. Fultz S C et al. *Phys. Rev.* **127** 1273 (1962)
72. Berman B L, Fultz S C *Rev. Mod. Phys.* **47** 713 (1975)
73. Dietrich S S, Berman B L *Atom. Data Nucl. Data Tabl.* **38** 199 (1988)
74. Bogdankevich O V *Sov. Atom. Energ.* **12** 208 (1962); *Atom. Energ.* **12** 198 (1962)
75. Kapitonov I M, Thesis for Doct. Phys.-Math. Sci. (Moscow: Skobeltsyn Institute of Nuclear Physics, Lomonosov Moscow State Univ., 1983)
76. Ishkhanov B S et al. "Konfiguratsionnoe rasshcheplenie dipol'nogo gigantskogo rezonansa v atomnykh yadrakh", Preprint No. 578 (Moscow: Institute for Nuclear Research, Academy of Sciences of the Soviet Union, 1978)
77. Ishkhanov B S, Kapitonov I M, Eramzhyan R A *Sov. J. Part. Nucl.* **23** 774 (1992); *Fiz. Elem. Chast. At. Yad.* **23** 1770 (1992)
78. Varlamov V V et al. "Tsentr dannykh fotoyadernykh eksperimentov" *Gos. Sluzhba Standart. Spravochnykh Dannykh. Inform. Byull.* (7) 12 (1978)
79. Lomonosov Moscow State Univ. Skobeltsyn Institute of Nuclear Physics. Centre for Photonuclear Experiments Data. Nuclear Reaction Database (EXFOR), http://cdfe.sinp.msu.ru/exfor/index.php
80. Varlamov A V et al. "Atlas of giant dipole resonances. Parameters and graphs of photonuclear reaction cross sections", Work performed under the Coordinated Research Project "Compilation and Evaluation of Photonuclear Data for Applications" INDC(NDS)-394 (Vienna: IAEA Nuclear Data Section, 1999)
81. International Atomic Energy Agency. Nuclear Data Service. NRDC "Experimental Nuclear Reaction Data (EXFOR)", https://www-nds.iaea.org/exfor/
82. USA National Nuclear Data Center. Database "CSISRS and EXFOR Nuclear Reaction Experimental Data"
83. Ahrens J et al. *Nucl. Phys. A* **251** 479 (1975)
84. Singh P P et al. *Nucl. Phys.* **65** 577 (1965)
85. Ishkhanov B S, Kanzyuba V G, Orlin V N *Yad. Fiz.* **40** 9 (1984)
86. Varlamov V V et al. *Yad. Fiz.* **30** 1185 (1979)
87. Bogdanova N A et al. *Vestn. Mosk. Univ. Ser. Fiz. Astron.* **28** 16 (1987)
88. Fallieros S, Goulard B *Nucl. Phys. A* **147** 593 (1970)
89. Akyüz R Ö, Fallieros S *Phys. Rev. Lett.* **27** 1016 (1971)
90. McNeill K G et al. *Phys. Rev. C* **47** 1108 (1993)
91. Kapitonov I M *Bull. Russ. Acad. Sci. Phys.* **79** 526 (2015); *Izv. Ross. Akad. Nauk. Fiz.* **79** 569 (2015)
92. Speth J, van der Woude A *Rep. Prog. Phys.* **44** 719 (1981)
93. Van Der Woude A *Prog. Part. Nucl. Phys.* **18** 217 (1987)
94. Harakeh M N, van der Woude A *Giant Resonances: Fundamental High-Frequency Modes of Nuclear Excitation* (Oxford: Oxford Univ. Press, 2001)
95. Chakrabarty D R, Dinh Dang N, Datar V M *Eur. Phys. J. A* **52** 143 (2016)
96. Lukirskii A P, Britov I A, Zimkina T M *Opt. Spectrosc.* **17** 234 (1964); *Opt. Spektrosk.* **17** 438 (1964)
97. Ederer D L *Phys. Rev. Lett.* **13** 760 (1964)
98. Samson J L *Adv. Atom. Mol. Phys.* **2** 178 (1966)

99. Zimkina T M et al. *Sov. Phys. Solid State* **9** 1128 (1967); *Fiz. Tverd. Tela* **9** 1447 (1967); *Sov. Phys. Solid State* **9** 1163 (1967); *Fiz. Tverd. Tela* **9** 1490 (1967)
100. de Heer W A et al. *Phys. Rev. Lett.* **59** 1805 (1987)
101. Hoheisel W et al. *Phys. Rev. Lett.* **60** 1649 (1988)
102. Tiggesbäumker J et al. *Chem. Phys. Lett.* **190** 42 (1992)
103. Gensterblum G et al. *Phys. Rev. Lett.* **67** 2171 (1991)
104. Hertel I V et al. *Phys. Rev. Lett.* **68** 784 (1992)
105. Wendin G *Phys. Lett. A* **46** 119 (1973)
106. Sairanen O-P, Aksela S, Kivimaki A *J. Phys. Condens. Matter* **3** 8707 (1991)
107. Kafle B P et al. *J. Phys. Soc. Jpn.* **77** 014302 (2008)
108. Nesterenko V O *Fiz. Elem. Chast. At. Yad.* **23** 1667 (1992)
109. Bertsch G F, Tománek D *Phys. Rev. B* **40** 2749 (1989)
110. Kaplan I G, Mondragon A, Smirnov Yu F *Rev. Mexicana Fisica* **42** (Suppl. 1) 117 (1995)